Potentiostatic Electrodeposition of Ti–Al Alloy with 40% Titanium from the Lewis Acidic 1-Butyl-3-Methylimidazolium Chloride-Aluminum Chloride Ionic Liquid Electrolyte

Pravin S. Shinde, Yuxiang Peng, and Ramana G. Reddy

Abstract Ti–Al alloys were electrodeposited from the Lewis acidic electrolyte containing 1-butyl-3-methylimidazolium chloride (BMIC) ionic liquid (IL) and aluminum chloride ($AlCl_3$). Constant potential electrodeposition was performed in a two-electrode configuration on copper cathode for 4 h at 383 K from BMIC-$AlCl_3$ electrolyte with a fixed $AlCl_3$ mole fraction and deposition potential. Titanium was served as an anode and also the source of Ti ions. Ti–Al alloys deposited on Cu substrate at different synthesis conditions were analyzed using scanning electron microscopy, energy-dispersive X-ray spectroscopy, and X-ray diffraction techniques. A $Ti_{0.4}Al_{0.6}$ phase with 40-atom % Ti was obtained in the final deposit at optimized process parameters and was confirmed by repeating electrodeposition experiments with identical synthesis conditions. After each electrolysis experiment, the Cu cathode weight gain and Ti anode weight loss were measured to determine the Faradaic current efficiency of the Ti–Al electrodeposition process. The current efficiency and energy consumption values were 49.93 ± 0.95 and 23.77 ± 0.89 kWh kg^{-1}, respectively.

Keywords Ti–Al alloy · BMIC-$AlCl_3$ ionic liquid · Potentiostatic Electrolysis

Introduction

Titanium (Ti) production by the Kroll process has been the longest known primary method [1], which is an expensive process due to the difficulty of extracting and machining the Ti [2]. Therefore, Ti is usually obtained in the form of alloys. Ti and its alloys (Al, Mo, and Fe) find potential applications in aerospace (aircraft, spacecraft, and missiles) and medical (bone-compatible and surgical tools) industries because of their greater strength-to-weight ratio, excellent corrosion-resistant

---

P. S. Shinde · Y. Peng · R. G. Reddy (✉)
Department of Metallurgical and Materials Engineering, The University of Alabama, Tuscaloosa, AL 35487, USA
e-mail: rreddy@eng.ua.edu

TMS 2022 151st Annual Meeting & Exhibition Supplemental Proceedings,
The Minerals, Metals & Materials Series,
https://doi.org/10.1007/978-3-030-92381-5_8

properties [3–6]. Electrodeposition has been regarded as one of the inexpensive technologies for the deposition of alloy coatings. Electrochemical synthesis of Ti metal or its alloys from low-temperature ionic liquid (IL) electrolytes is one of the fascinating methods [7]. However, the electrodeposition of pure Ti is challenging compared to other metals like aluminum because of its different oxidation states (II, III, and IV). The synthesis of Ti in the form of Ti–Al alloy from ionic liquids is particularly promising as $AlCl_3$ can easily form eutectic composition at room temperature and increase the electrolyte's conductivity. The molten chloride salt electrolytes have been employed to electrodeposit of Ti and Ti–Al alloys via an energy-efficient and cost-effective extraction process [8–12]. Several attempts have been made to understand the electrochemistry of Ti ions in the ionic liquid electrolytes to improve the Ti–rich deposition of Ti–Al alloy [13–21]. All the attempts of obtaining pure Ti resulted in the co-deposition of Al and Ti. Nevertheless, the low-temperature electrodeposition of Ti–Al alloys using ionic liquid electrolyte is not only energy-efficient but also eliminates high-temperature melting and consolidation processes.

The percentage of Ti in the Ti–Al alloy varies depending on the concentration of Ti species, the Lewis acidity, electrolyte type, and the applied electrochemical potential/current density. About 28 at.% Ti was obtained from NaCl:$AlCl_3$ (1:2 mol ratio) melts at 423 K containing Ti^{2+} ions, which were electrochemically dissolved by varying the Ti(II) concentration and the applied current. Potentiostatic deposition of Al–Ti on the GC electrode from equimolar $AlCl_3$-NaCl melt containing anodically dissolved Ti at −0.085 V versus Al/Al(III) for 2 h resulted in different alloys $AlTi_3$, Al_2Ti, and Al_3Ti alloys, with $AlTi_3$ dominating at a lower temperature (473 K) and Al_2Ti dominating at a higher temperature (573 K). EDS suggested Ti content in the range of 12.6–21.9 at.% [22]. The Al–Ti alloy electrodeposited from $AlCl_3$-NaCl-KCl eutectic molten salt electrolyte in a flowing cell at 473 K improved with the addition of $TiCl_3$, resulting in a smooth deposit of 40.2% Ti content at current density as high as 200 mA cm^{-2}. Ti co-deposition could only proceed in the presence of Ti^{2+} species in the electrolyte that were obtained by reducing Ti^{3+} with the help of Al powder [23]. Al–Ti alloy with 1 wt.% Ti was obtained using TiO_2 feeds at high temperatures (1233–1253 K) during aluminum electrolysis for 4 h from fluoride-based melts at a cathodic current density of 900 mA cm^{-2} and a NaF-AlF_3 cryolite ratio of 2.2 [24]. About 24.1 at.% Ti was obtained from NaCl:$AlCl_3$ (1:2 mol ratio) melts at 423 K containing Ti^{2+} ions, which were electrochemically dissolved by varying the Ti(II) concentration and/or the applied current [12, 25]. The constant potential (−1.5 V vs. Pt) and constant current (10 mA cm^{-2}) electrolysis from EMIC-$AlCl_3$ (1:2 mol ratio) at 383 K for 1-h duration resulted in Ti deposits of 14 at.% and 16.5 at.%, respectively. Relatively higher Ti content for later was attributed to the relatively higher concentration of Ti species [17]. Stafford et al. reported about 18.4 at.% Ti by electrodeposition from chloroaluminate EMIC-$AlCl_3$ electrolyte containing Ti^{2+} concentration of 170 mmol L^{-1} at 353 K [26]. Tsuda et al. studied electrochemistry and the dissolution effect of different Ti ions (Ti^{2+}, Ti^{3+}, and Ti^{4+}) in EMIC-$AlCl_3$ melts with $AlCl_3$ mole fractions of 0.6 and 0.667 on the electrodeposition of Al–Ti alloys. Ti content in Ti–Al alloy obtained at the $AlCl_3$ mole fraction of 0.667 by dissolving 150 mmol L^{-1} of Ti^{2+} species in EMIC-$AlCl_3$

at 353 K was 19.1 at.% at a current density of 2.5 mA cm^{-2} and decreased to 12.4 at.% with further increase of current density to 20 mA cm^{-2} [20].

Ti–Al deposits obtained from BMIC-$AlCl_3$ (1:2 molar ratio) electrolyte at 373 K appears to be smooth and dendrite-free at relatively low potentials (−1 to −1.3 V vs. Ti) for 1 h, however, results in with lower Ti content (3 at.%), due to lower electrochemically dissolved Ti concentration at lower applied potential [14]. Electrodeposition of dense and adhesive Ti–Al alloy coatings are reported on mild steel from BMIC-$AlCl_3$ ionic liquid electrolyte containing $TiCl_4$ at 343 K. The composition, microstructure of obtained Ti–Al coatings depended on the applied current density and $TiCl_4$ concentration. The Ti concentration in the Ti–Al coatings increased to an optimum level of 11.4 at.% for 0.22 mol L^{-1} $TiCl_4$ as evidenced from XRD studies [27]. Ti content decreased at higher current densities beyond 5 mA cm^{-2}, corroborating a similar phenomenon observed by Tsuda et al. [20]. Thus, the primary electrodeposition process proceeds at more negative potentials to deposit microcrystalline or bulk Ti–Al alloy.

In our previous study, the chronopotentiometric electrodeposition of Ti–Al alloy was achieved from BMIC-$AlCl_3$ (1:2 molar ratio) electrolyte at 373 K at different current densities (13.5–89.1 mA cm^{-2}) for 4 h. The obtained Ti–Al consisted of compact and dendritic deposits with disordered face-centered cubic (FCC) lattice containing 14.56–20.75 at.% Ti [28]. Electrodeposition of Ti–Al alloys was further investigated from the BMIC-$AlCl_3$ (1:2 molar ratio) system by including Ti^{4+} ions (0.019 molar ratio of $TiCl_4$) at different temperatures in the range of 343–498 K and at various potentials in the range of 1.5–3.0 V. Ti–Al alloys with 15–27 at.% Ti contents were produced with current efficiencies in the range of 25–38%. Higher potentials (2.5–3.0 V) and higher temperatures (373–398 K) resulted in non-uniform and coarse-grained Ti–Al deposits. Lower potentials (1.5–2.5 V) produced smooth, bright, and finer particle-sized Ti–Al alloys. The estimated energy consumption of Ti–Al alloys production varied from 16.63 to 31.98 kWh kg^{-1} of Ti–Al alloy [19, 29]. Motivated from these results, these studies were revisited. Ti content in the Ti–Al alloy was observed to be interdependent regardless of $TiCl_4$ addition because sufficient Ti ions are electrochemically dissolved in the ionic liquid electrolyte at higher electrochemical potential and electrolysis duration.

In this work, Ti–rich Ti–Al alloy is deposited on copper substrate by constant-potential electrolysis from the Lewis acidic ionic liquid mixture of 1-butyl-3-methylimidazolium chloride and aluminum chloride (BMIC-$AlCl_3$) using the electrochemical dissolution of Ti anode. This research work is aimed to obtain the optimum percentage of Ti in the Ti–Al alloy at optimum deposition potential, duration, and the molar ratio of BMIC ionic liquid and $AlCl_3$. The electrodeposited material is characterized by XRD and SEM-SEM to yield 40 at.% Ti in the final Ti–Al deposit.

Experimental

Preparation of BMIC-AlCl$_3$ Ionic Liquid Electrolyte

The chemicals such as anhydrous aluminum chloride ($AlCl_3$, 95%, Alfa Aesar) and 1-butyl-3-methyl imidazolium chloride (BMIC, 98%, Sigma Aldrich) ionic liquid were purchased and used without further treatment. The copper sheet (99%, 0.25 cm thick) was purchased from Sigma Aldrich. A pure titanium sheet (2 mm thick, 99.99%) was obtained from Alfa Aesar®. The ultrahigh pure (UHP) argon gas (99.999%) was obtained from Airgas. All chemical reagents were handled in a dry atmosphere. The eutectic mixture of Lewis acidic BMIC-$AlCl_3$ electrolyte was prepared by mixing a 1:2 molar ratio ($AlCl_3$ mole fraction, $X_{AlCl3} = 0.667$) of BMIC IL and $AlCl_3$ in a Pyrex beaker at room temperature under constant stirring for 30 min until a clear homogeneous solution was obtained. $X_{AlCl3} = 0.667$ was chosen to maximize the concentration of $Al_2Cl_7^-$ anion species crucial for metal electrodeposition from the BMIC-$AlCl_3$ electrolyte. The desired amount of clear electrolyte was then transferred to the 50 mL electrochemical Pyrex cell placed on a hot plate, and the electrolyte was stirred for several minutes using a magnetic stirrer at 120 RPM to achieve a stable temperature of 383 K for electrochemical deposition.

Electrochemical Deposition

The electrodeposition experiments were performed at constant potential from BMIC-$AlCl_3$ electrolyte at 383 K using a KEPCO power supply and a KEITHLEY multimeter controlled by LabVIEW software. The electrochemical cell for the measurements consisted of a 40 mL Pyrex® glass beaker fitted with Teflon/Perspex cover, which has provisions for inserting the electrodes, thermometer, and inert gas inlet/outlets shown schematically in Fig. 1. The Ti ions were incorporated in the BMIC-$AlCl_3$ electrolyte from the Ti anode electrode during electrolysis. The source of Al ions was from $AlCl_3$. The two-electrode electrolysis setup consisted of a copper sheet (2 × 2 × ~0.25 cm, 99%, Sigma Aldrich) as working electrode (WE) and a Ti plate (2 × 2 × ~2 cm, 99.99%, Alfa Aesar®) as the counter electrode (CE). The working distance between WE and CE was kept constant at 2 cm. The constant potential electrolysis experiments were performed and repeated at least three times for 4 h duration. The temperature of the hot plate was precisely controlled and monitored by the inserted thermometer. The Ar gas flow was continuously maintained over the electrolyte's surface throughout the experiment (through the alumina tube).

Before the electrolysis experiment, both the Cu and Ti electrodes were polished with 800-grit SiC abrasive paper, rinsed thoroughly with deionized water, cleaned in an ultrasonic bath for 5 min, and dried by air to remove any residual impurities. The height of the electrodes immersed in the BMIC-$AlCl_3$ electrolyte was measured after each experiment for efficiency and energy consumption calculations. Ti–Al

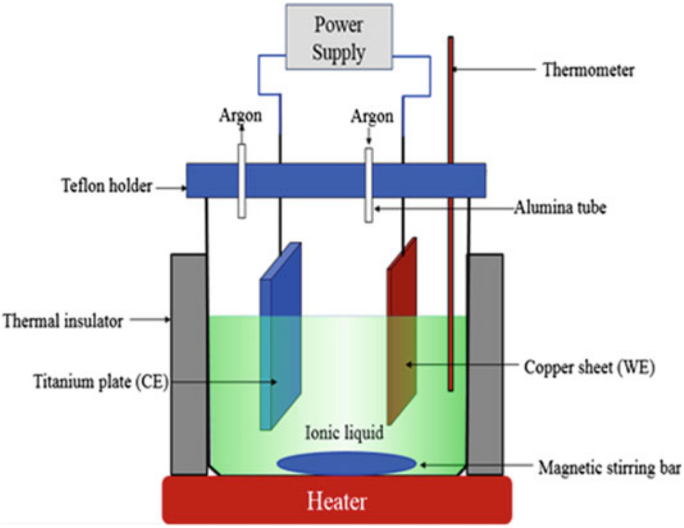

Fig. 1 Schematic of a two-electrode experimental setup for electrolysis from BMIC-$AlCl_3$ electrolyte

alloy was deposited on copper plate by constant potential electrolysis from BMIC-$AlCl_3$ ($X_{AlCl3} = 0.667$) electrolyte at 383 K at a fixed applied potential of −3.0 V for 4 h duration. The electrodeposited Ti–Al deposits obtained on Cu electrodes were characterized using structural, morphological, and compositional techniques such as scanning electron microscopy (SEM) on Thermo Scientific™ Apreo scanning electron microscope equipped with energy-dispersive spectroscopy (EDS), and X-ray diffraction (XRD) on a Bruker D8 Discover X-ray diffractometer with GADDS by employing monochromatic Co Kα radiation.

Results and Discussion

Constant Potential Electrodeposition of Ti–Al from BMIC-$AlCl_3$ Electrolyte

The Ti–Al electrodeposits were obtained from BMIC-$AlCl_3$ electrolyte at constant potential conditions for a 4-h duration at electrolyte temperature of 383 K and electrolyte rotation speed of 120 rpm. The constant-potential experiments were performed and repeated at least three times at identical conditions to check the reproducibility of results (morphology, composition, current efficiency, and energy consumption). The preparation of ionic liquid, polishing, and cleaning of electrodes were done identically. The electrode size, electrode separation distance, depth of

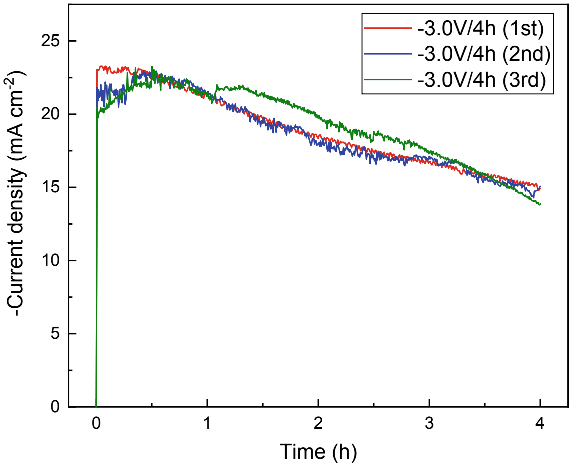

Fig. 2 The current density-time plots for 2-electrode electrolysis for 4 h using KEPCO power supply at a constant potential of –3.0 V from BMIC-$AlCl_3$ electrolyte at 383 K

electrode immersion, and electrolyte volume (30 mL) were all the same for all the experiments. To rule out differences in electrolyte composition, the sufficient stock solution of electrolyte with $AlCl_3$ mole fraction of 0.667 was prepared in a bulk quantity and stored correctly to avoid contamination. A 30 mL of electrolyte was taken from this stock solution for all sets of experiments. All the samples were then analyzed by XRD, SEM, and EDS to determine the phase, morphology, uniformity, and elemental composition of the synthesized Ti–Al deposits. The Ti ions were incorporated in-situ into the BMIC-$AlCl_3$ ionic liquid by electrochemical dissolution of the Ti anode during the 4-h electrolysis experiment. The Cu cathode and Ti anode electrodes were weighed before and after each electrolysis experiment to account for Ti ions stripped from the Ti anode and the amount of Ti–Al material deposited onto the Cu cathode electrode.

Figure 2 shows current density-time plots recorded from 2-electrode electrolysis from BMIC-$AlCl_3$ ($AlCl_3$ mole fraction of 0.667) electrolyte by applying a constant potential of −3.0 V for 4 h at 383 K and with electrolyte flow of 120 rpm. The electrochemical deposition of Al from such chloroaluminate ionic liquid electrolytes has been reported to be mainly due to contribution from the diffusion of $Al_2Cl_7^-$ species [30–32]. The initial current density is driven by the $Al_2Cl_7^-$ ions in the ionic liquid electrolyte leading to the reduction of aluminum atoms. Once the Ti ions are anodically dissolved into the electrolyte, they form a complex with $Al_2Cl_7^-$ ions to obtain $Ti[(Al_2Cl_7)_4]^{2-}$ complex. The possible reaction mechanisms of co-deposition of Al and Ti have been reported previously [14]. In short, the co-deposition of 3-electron reduction of Al and 2-electron reduction of Ti proceeds according to the reactions (1, 2):

$$4[Al_2Cl_7]^- + 3e^- \leftrightarrow \text{Al (At Cathode)} + 7[AlCl_4]^- \quad (1)$$

$$\left[Ti(Al_2Cl_7)_4\right]^{2-} + 2e^- \leftrightarrow \text{Ti (At Cathode)} + 4[Al_2Cl_7]^- \quad (2)$$

Table 1 The weight gain of Ti–Al deposit on Cu cathode, the weight loss of Ti ions from Ti anode, Faradaic efficiency, and the energy consumption values for 4-h constant potential electrolysis at −3.0V from BMIC-$AlCl_3$ electrolyte at 383 K at 120 RPM

Potential	−3 V (1st)	−3 V (2nd)	−3 V (3rd)
Total charge (C)	2348	1915	2003
Total atomic weight (g mol^{-1})	35.336	35.336	35.336
Total electron transferred	2.600	2.600	2.600
Theoretical weight gain (g)	0.331	0.270	0.282
Actual weight gain (g)	0.162	0.139	0.139
Initial current density, $J_{t=0\ h}$ (mA cm^{-2})	−23.04	−21.83	−20.48
Current density after 4 h, $J_{t=4\ h}$ (mA cm^{-2})	−14.92	−15.06	−13.87
Efficiency (%)	48.98	51.53	49.27
Energy consumption (kWh kg^{-1})	24.66	22.28	24.37
Ti anode weight loss	0.306	0.257	0.264

Initially, the current density (in Fig. 2) reaches a maximum (in the range of 22–24 mA cm^{-2}). It then decreases to ~15 mA cm^{-2} over time for all the repeated experiments at the end of 4 h electrolysis. The average current density for three electrodes is ~18 mA cm^{-2}. The decrease in current density over time could be due to lower diffusivity and availability of electroactive species ($Al_2Cl_7^-$ or Ti-complex) in the vicinity of the electrode surface. Table 1 shows the weight loss and gain measured for Ti anode and Cu cathode for three experiments.

The weight gain of Cu cathode increases with electrolysis time due to the deposition of Ti–Al. At the same time, the Ti ions released by Ti anode in BMIC-$AlCl_3$ electrolyte also increases with time, as indicated by weight loss of Ti anode. Interestingly, the amount of Ti ions dissolved from the Ti anode is more significant than the percentage of Ti in the electrodeposited Ti–Al material (coating on Cu^+ stripped powder). Although a higher concentration of Ti ions is released in electrolyte upon anodic dissolution of Ti anode, significantly fewer $Ti[(Al_2Cl_7)_4]^{2-}$ ions are available for electrodeposition as there may be a saturation limit at equilibrium to form the Ti-complex with $Al_2Cl_7^-$ ions. As a result, there is a drop in current density over the electrolysis time. The current efficiency and energy consumption values align with our previously published reports [19, 29].

Characterization of Ti–Al Deposits by XRD and SEM-EDS

The Ti–Al electrodeposits are characterized by XRD to determine the alloy composition. Figure 3 shows the normalized XRD patterns of Ti–Al electrodeposits on Cu substrate. All the Ti–Al deposits are crystalline and show five distinct crystallographic peaks (dark circles) such as (111), (200), (220), (311), and (222) belonging to the $Ti_{0.40}Al_{0.60}$ phase of Ti–Al alloy with the cubic crystal structure (space group:

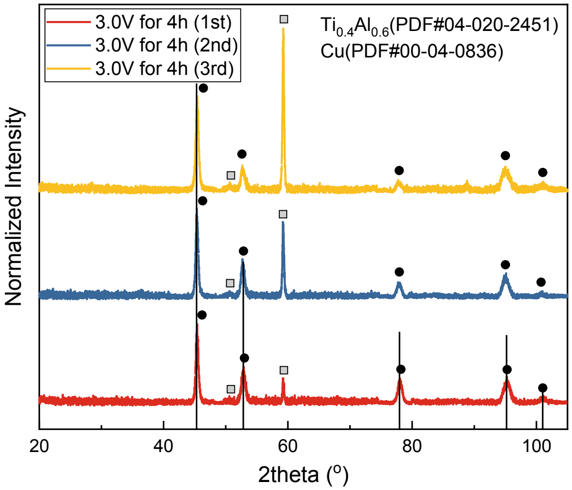

Fig. 3 XRD patterns of Ti–Al electrodeposits obtained from BMIC-$AlCl_3$ on copper substrate by 2-electrode-electrolysis at 383 K using KEPCO power supply at −3.0 V for 4 h for three repeated experiments (Electrodes: 1st, 2nd, and 3rd). The vertical lines represent the lines from standard diffraction patterns of Ti–Al ($Ti_{0.40}Al_{0.60}$) and Cu

Fm-3 m (225), lattice parameter, *a*: 4.022 Å) as identified according to PDF4+ card (ICDD#:04-020-2451). The rest of the peaks (open squares) are due to the copper substrate (ICDD#:00-04-0836), and no other impurity or low-titanium Ti–Al alloy phases are seen. This suggests that Ti–Al electrodeposits obtained at − 3.0 V are reproducible, producing 40 at.% Ti.

The SEM and EDS analyses were performed to examine the surface morphology and chemical composition of the electrodeposits. Figure 4 (left) shows the surface morphology of Ti–Al deposits on copper substrates obtained by constant potential electrolysis from BMIC-$AlCl_3$ electrolyte at − 3.0 V for 4 h at 383 K.

The morphology of Ti–Al deposits is uniform and porous. The Ti–Al growth is dendritic with uniformly covered spherical grains (20–25 μm) enclosing the smaller grains. The spherical grains break open over a prolonged period of electrolysis time. On top of the dendritic growth of spherical grains, few white overgrowths are crystallized. Such crystallization could be due to a slight rise in temperature of the

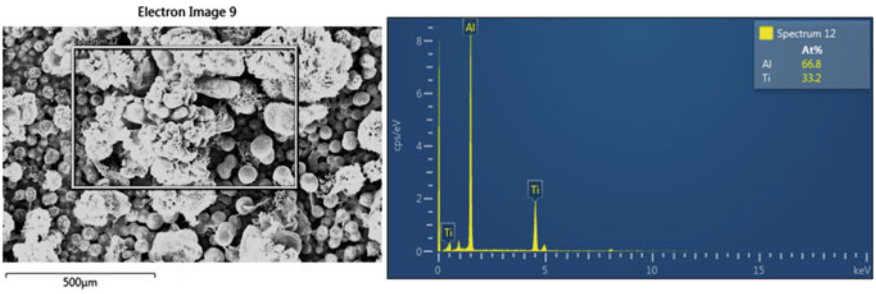

Fig. 4 Surface morphology and composition of representative Ti–Al alloy coating obtained on Cu substrate by constant-potential electrodeposition from BMIC-$AlCl_3$ (1:2) at −3.0 V for 4 h

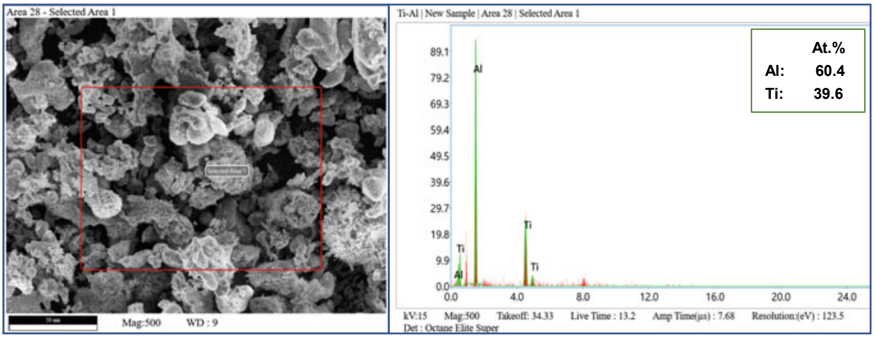

Fig. 5 Surface morphology and composition of representative Ti–Al alloy powder collected by scrapping/stripping the Ti–Al coating from the Cu substrate

BMIC-$AlCl_3$ electrolyte leading to accumulation of diffused species of Al as well as Ti, eventually covering few regions of the Ti–Al deposits. Due to their porous nature and large surface area, these overgrowths appear to trap the anions, especially Ti-complex ions. Figure 4 (right) shows the representative EDS spectrum of Ti–Al deposit, revealing the chemical compositions of Ti and Al in Ti–Al electrodeposit to be 33.2 at.% and 66.8 at.%, respectively. It should be noted that the obtained values are not precisely accurate due to the semi-quantitative nature of the EDS measurement.

The SEM–EDS analysis was also performed on the powders stripped/scraped from the Cu substrate, and the Ti content was close to 40% (38.9 ± 0.5 at.%), as shown in Fig. 5. Thus atomic percentage composition observed from SEM–EDS agrees reasonably with the XRD studies.

Calculation of Current Efficiency and Energy Consumption

The weight gain of Ti–Al deposit on Cu cathode, the weight loss of Ti ions from Ti anode, Faradaic efficiency, and the energy consumption values shown earlier in Table 1 are calculated according to the procedure discussed below. The total weight of Ti–Al that included the weight of Ti–Al powder stripped and Ti–Al deposit on Cu substrate itself was considered for efficiency and energy consumption calculations. The cathodic current efficiency represents how efficiently the applied electricity is utilized to deposit the metals and is defined as the percentage of the weight gain of the electrodeposit relating to the actual Ti–Al alloy produced to the Ti–Al alloy that would theoretically be obtained based on Faraday's law. The current efficiency (η) is calculated using Eq. (3).

$$\Delta = \frac{\Delta W}{W_t} \times 100\% \quad (3)$$

The experimental weight gain (ΔW) was obtained by adding the weight difference of the cathode before and after electrodeposition, and the weight of the precipitate/powder stripped off from the cathode during the electrolysis/cleaning process. The theoretical weight gain (W_t) of the deposit is calculated using Faraday's law, given by Eq. (4).

$$W_t = \frac{jtaA}{nF} = \frac{Qa}{nF} \tag{4}$$

where j is the current density (A cm^{-2}), t is time (s), a is the total weight of all the atoms in the deposit (g mol^{-1}), A is the area of the electroactive region on the working electrode (cm^2), n is the total number of transferred electrons, and F is Faraday constant. Since current density is not a constant during the electrodeposition process, the total charge (Q), a product ($j \times$ t) for a given area A, is obtained by integrating the current versus time plot in Fig. 2 using Eq. (5).

$$\mathrm{Q} = \int_0^t A \times j dt \tag{5}$$

The total atomic weight (Al and Ti) and the total number of transferred electrons involving the reduction of Al and Ti are calculated based on the final composition of Ti and Al using Eqs. (6, 7).

$$a_{total} = a_{Al} \times X_{Al} + a_{Ti} \times X_{Ti} \tag{6}$$

$$n_{total} = n_{Al} \times X_{Al} + n_{Ti} \times X_{Ti} \tag{7}$$

where a_{total} is the total weight of Al and Ti atoms, n_{total} is the total number of transferred electrons, a_{Al} is the atomic weight of Al (26.982 g mol^{-1}), a_{Ti} is the atomic weight of Ti (47.867 g mol^{-1}), n_{Al} is electrons transferred for producing 1 mol of Al (3), n_{Ti} is electrons transferred for producing 1 mol of Ti (2), X_{Al} and X_{Ti} are the corresponding atomic fractions of Al and Ti in the final Ti–Al deposit obtained from XRD.

The energy consumption, E (kWh kg^{-1}), of the electrodeposition process, is then determined using Eq. (8).

$$E = \frac{V \times Q}{\Delta \times \Delta \mathrm{W}} \tag{8}$$

where V is the applied potential, Q is the total charge (Coulomb or Ampere second) calculated from Eq. (5).

Thus, through this work, it is demonstrated that it is feasible to synthesize Ti–Al alloy with as high as 40 at.% Ti by low-temperature electrolysis from BMIC-$AlCl_3$ ionic liquid electrolyte at relatively lower deposition potential by the in-situ electrochemical anodic dissolution of Ti ions from Ti anode during electrolysis.

Conclusions

Electrodeposition of Ti–Al alloy with 40% Ti was accomplished for the first time from the Lewis acidic electrolyte containing 1-butyl-3-methylimidazolium chloride (BMIC) ionic liquid and aluminum chloride ($AlCl_3$) with a 0.667-mol fraction of $AlCl_3$. The Ti–Al electrodeposits were obtained on Cu substrate by employing a constant potential of -3.0 V for 4 h in a two-electrode configuration at 383 K from BMIC-$AlCl_3$ electrolyte. Both XRD and SEM–EDS confirmed the formation of crystalline $Ti_{0.4}Al_{0.6}$ phase with cubic crystal structure on Cu. Three identical 4-electrolysis experiments confirmed the repeatability of producing 40-at.% Ti in the Ti–Al electrodeposit. The morphology of Ti–Al deposits consisted of uniform coverage of spherical grains with dendritic growth with few white overgrowths. The Faradaic current efficiency and energy consumption values of the Ti–Al electrodeposition process were obtained using cathode weight gain, anode weight loss, and the concentration of Ti obtained from XRD. The current efficiency and energy consumption values were 49.93 ± 0.95 and 23.77 ± 0.89 kWh kg^{-1}, respectively. More work is underway further to improve the percentage of Ti in the Ti–Al deposits.

Acknowledgements The authors acknowledge the financial support from the National Science Foundation (NSF) award number 1762522 and ACIPCO for this research project. The authors also thank the Department of Metallurgical and Materials Engineering, The University of Alabama, for providing the experimental and analytical facilities.

References

1. Kroll W (1940) The production of ductile titanium. Trans Electrochem Soc 78:35
2. Crowley G (2003) How to extract low-cost titanium. Adv Mater Processes 161:25–27
3. Inagaki I, Takechi T, Shirai Y, Ariyasu N (2014) Application and features of titanium for the aerospace industry. Nippon Steel Sumitomo Metal Tech Rep 106:22–27
4. Peters M, Kumpfert J, Ward CH, Leyens C (2003) Titanium alloys for aerospace applications. Adv Eng Mater 5:419–427
5. Elias C, Lima J, Valiev R, Meyers M (2008) Biomedical applications of titanium and its alloys. Jom 60:46–49
6. Niinomi M, Nakai M, Hieda J, Cho K, Akahori T, Hattori T et al (2013) Research and development of low-cost titanium alloys for biomedical applications. Key Engineering Materials: Trans Tech Publ, pp 133–139
7. Zhang M, Kamavaram V, Reddy RG (2006) Ionic liquid metallurgy: novel electrolytes for metals extraction and refining technology. Mining Metall Explor 23:177–186
8. Fung KW, Mamantov G (1972) Electrochemistry of titanium (II) in $AlCl_3$-NaCl melts. J Electroanal Chem 35:27–34
9. Girginov A, Tzvetkoff TZ, Bojinov M (1995) Electrodeposition of refractory-metals (Ti, Zr, Nb, Ta) from molten-salt electrolytes. J Appl Electrochem 25:993–1003
10. Rolland W, Sterten A, Thonstad J (1987) Electrodeposition of titanium from chloride melts. Proc—Electrochem Soc 1987–7:775–785

11. Head RB (1961) Electrolytic production of sintered titanium from titanium tetrachloride at a contact cathode. J Electrochem Soc 108:806–809
12. Stafford GR (1994) The electrodeposition of Al_3Ti from chloroaluminate electrolytes. J Electrochem Soc 141:945–953
13. Shinde P, Peng Y, Reddy RG (2020) Electroanalytical study of active species to deposit ti alloy from 1-butyl-3-methylimidazolium chloride-aluminum chloride ionic liquid. ECS Trans 98:231–243
14. Shinde PS, Peng Y, Reddy RG (2020) Electrodeposition of titanium aluminide (TiAl) alloy from $AlCl_3$-BMIC ionic liquid at low temperature. Springer International Publishing, Cham, pp 1659–1667
15. Bogala MR (2015) Electrodeposition of titanium aluminides from aluminum chloride: 1-butyl-3-methyl imidazolium chloride ionic liquid. University of Alabama Libraries
16. Reddy RG, Shinde PS, Liu A (2021) The emerging technologies for producing low-cost titanium. J Electrochem Soc
17. Shinde PS, Reddy RG (2021) Effect of dissolution of titanium ions on Ti alloys electrodeposition from EMIC-$AlCl_3$ ionic liquid at low temperature. Springer International Publishing, Cham, pp 141–153
18. Stafford GR, Moffat TP (1995) Electrochemistry of titanium in molten $2AlCl_3$-NaCl. J Electrochem Soc 142:3288–3296
19. Pradhan D, Reddy R, Lahiri A (2009) Low-temperature production of Ti-Al alloys using ionic liquid electrolytes: effect of process variables on current density, current efficiency, and deposit morphology. Metall Mater Trans B 40:114–122
20. Tsuda T, Hussey CL, Stafford GR, Bonevich JE (2003) Electrochemistry of titanium and the electrodeposition of Al-Ti alloys in the lewis acidic aluminum chloride-1-Ethyl-3-methylimidazolium chloride melt. J Electrochem Soc 150:C234–C243
21. Endres F, Zein El Abedin S, Saad AY, Moustafa EM, Borissenko N, Price WE et al (2008) On the electrodeposition of titanium in ionic liquids. Phys Chem Chem Phys 10:2189–2199
22. Cvetković VS, Vukićević NM, Milićević-Neumann K, Stopić S, Friedrich B, Jovićević JN (2020) Electrochemical deposition of Al-Ti alloys from equimolar AlCl3 + NaCl containing electrochemically dissolved titanium. Metals 10:88
23. Uchida J-I, Seto H, Shibuya A (1995) Electrodeposition of Al-Ti alloy from chloroaluminate bath. J Surface Finish Soc Jpn 46:1167–1172
24. Awayssa O, Saevarsdottir G, Meirbekova R, Haarberg GM (2021) Electrodeposition of aluminium-titanium alloys from molten fluoride-oxide electrolytes. Electrochem Commun 123:106919
25. Janowski G, Stafford GR (1992) The microstructure of electrodeposited titanium-aluminum alloys. Metall Trans A 23:2715–2723
26. Stafford GR, Tsuda T, Hussey C (2003) Order/disorder in electrodeposited aluminum-titanium alloys. J Min MetallSect B 39:23–42
27. Xu C, Hua Y, Zhang Q, Li J, Lei Z, Lu D (2017) Electrodeposition of Al-Ti alloy on mild steel from $AlCl_3$-BMIC ionic liquid. J Solid State Electrochem 21:1349–1356
28. Pradhan D, Reddy RG, Electrodeposition of titanium using BmimCl ionic liquid at higher cathode current densities. Unpublished work: Unpublished work, p 1
29. Pradhan D, Reddy RG (2009) Electrochemical production of Ti-Al alloys using $TiCl_4$-$AlCl_3$-1-butyl-3-methyl imidazolium chloride (BmimCl) electrolytes. Electrochim Acta 54:1874–1880
30. Pradhan D, Reddy RG (2014) Mechanistic study of Al electrodeposition from EMIC-$AlCl_3$ and BMIC-$AlCl_3$ electrolytes at low temperature. Mater Chem Phys 143:564–569

31. Jiang T, Chollier Brym MJ, Dubé G, Lasia A, Brisard GM (2006) Electrodeposition of aluminium from ionic liquids: Part I—electrodeposition and surface morphology of aluminium from aluminium chloride ($AlCl_3$)–1-ethyl-3-methylimidazolium chloride ([EMIm]Cl) ionic liquids. Surf Coat Technol 201:1–9
32. Tang J, Azumi K (2011) Optimization of pulsed electrodeposition of aluminum from AlCl3-1-ethyl-3-methylimidazolium chloride ionic liquid. Electrochim Acta 56:1130–1137